The Two Histidine Axial Ligands of the Primary Electron Donor Chlorophylls (P700) in Photosystem I Are Similarly Perturbed upon $P700^+$ Formation†

Jacques Breton,*,‡ Wu Xu,§,|| Bruce A. Diner,⊥ and Parag R. Chitnis§

Service de Bioénergétique, CEA-Saclay, 91191 Gif-sur-Yvette, France, Department of Biochemistry, Biophysics, and Molecular Biology, Iowa State University, Ames, Iowa 50011, and Central Research and Development Department, Experimental Station, E. I. du Pont de Nemours & Co., Wilmington, Delaware 19880-0173

Received June 4, 2002; Revised Manuscript Received July 16, 2002

ABSTRACT: The extent of delocalization of the positive charge in the oxidized dimer of chlorophyll (Chl) constituting P700, the primary electron donor of photosystem I (PSI), has been investigated by analyzing the perturbation upon $P700^+$ formation of infrared (IR) vibrational modes of the two His axial ligands of the two P700 Chl molecules. Fourier transform IR (FTIR) difference spectra of the photooxidation of P700 in PSI core complexes isolated from *Synechocystis* sp. PCC 6803 isotopically labeled either globally with ^{15}N or more specifically with ^{13}C on all the His residues reveal isotopic shifts of a differential signal at 1102/1108 cm^{-1}. This signal is assigned to a downshift upon $P700^+$ formation of the predominantly $C_5-N\tau$ imidazole stretching mode of His residue(s). The amplitude of this signal is reduced by approximately half in FTIR spectra of *Synechocystis* mutants in which His PsaB 651, the axial ligand to one of the two Chl molecules in P700, is replaced by Cys, Gln, or Leu. These observations provide further evidence that the positive charge in $P700^+$ is essentially delocalized over the two Chl molecules, in agreement with a previous FTIR study in which the frequency of the vibrational modes of the 9-keto and 10a-ester C═O groups of the two Chl's in P700, $P700^+$, and $^3P700$ were firmly established for the first time [Breton, J., et al. (1999) *Biochemistry 38*, 11585−11592]. Only limited perturbations of the amplitude and frequency of the 9-keto and 10a-ester C═O bands of the P700 Chl are elicited by the mutations. On the basis of comparable mutational studies of the primary electron donor in purple bacteria, these perturbations are attributed to small molecular rearrangements of the Chl macrocycle and substituents caused by the repositioning of the P700 dimer in the new protein cavity generated by the mutations. It is proposed that the perturbation of the FTIR spectra upon mutation of a His axial ligand of the P700 Chl recently reported in *Chlamydomonas reinhardtii* [Hastings, G., et al. (2001) *Biochemistry 40*, 12943−12949] can be explained by the same effect without the need for a new assignment of the C═O bands of P700. The distribution of charge/spin in $P700^+$ and $^3P700$ determined by FTIR spectroscopy is discussed in relation with the contrasting interpretations derived from recent magnetic resonance experiments.

The conversion of light energy into chemical energy by photosynthetic organisms occurs in membrane proteins called reaction centers (RC's)[1] and involves charge separation across the membrane. In the RC's, light-induced charge separation is initiated by special dimers of chlorophyll (Chl) or bacteriochlorophyll (BChl) molecules called primary electron donors (P). An electron is ejected from the excited state of the primary electron donor and reduces rapidly a sequence of electron acceptors positioned across the photosynthetic membrane and located at increasing distances from the primary donor. Owing to the central role of the primary donors in the photosynthetic processes, a wealth of spectroscopic techniques have been used to investigate their structure. Notably, a large number of optical, vibrational, and magnetic resonance spectroscopic techniques have been applied to the study of the electronic structure of the neutral, oxidized, and triplet states of primary electron donors in RC's of all the known classes of photosynthetic organisms (*1*). This has led to various models describing the organization of the (B)Chl molecules within the dimers, the interactions of the pigments with the surrounding protein, and the charge/spin distribution in the oxidized and triplet states of the primary donors. In the last two decades, advances in X-ray crystallography of membrane proteins have led to structural models of the RC's from purple photosynthetic bacteria (*2*−*4*) at resolutions approaching 2 Å (*5*, *6*). These models describe quite precisely the interaction of the non-hydrogen atoms of the BChl molecules of the primary electron donor with the nearby amino acid residues. Such structural information has led to the genetic engineering of a large number

† Part of this work was supported by grants to B.A.D. (NRICGP/USDA 97-35306-4882) and to P.R.C. (NSF MCB 0078268).

* To whom correspondence should be addressed. Phone: (331) 6908 2239. Fax: (331) 6908 8717. E-mail: cadara3@dsvidf.cea.fr.

‡ CEA-Saclay.

§ Iowa State University.

|| Current address: Department of Biochemistry, St. Jude Children's Hospital, 332 N. Lauderdale, Memphis, TN 38105.

⊥ E. I. du Pont de Nemours & Co.

[1] Abbreviations: Chl, (bacterio)chlorophyll; PSI, photosystem I; RC, reaction center; P, primary electron donor; FTIR, Fourier transform infrared; hfc, hyperfine coupling constant; *C.*, *Chlamydomonas*; *Rb.*, *Rhodobacter*; *S.*, *Synechococcus*; *Synechocystis*, *Synechocystis* sp. PCC 6803.

10.1021/bi0262404 CCC: $22.00
Published on Web 08/23/2002

of mutants with modified cofactor−protein interactions (*7*). These mutants have also been investigated with the spectroscopic techniques mentioned above, providing tests of the merits of these techniques for obtaining information on RC's whose structure is not available.

Besides the primary electron donor of purple photosynthetic bacteria, it is probably P700, the primary donor of photosystem I (PSI) of cyanobacteria, algae, and higher plants, that has been the most thoroughly investigated by structural and functional spectroscopy. Observations derived from optical spectroscopy provide strong evidence that P700 is a dimer of Chl molecules (*8*−*12*). On the other hand, the spin localization in $P700^+$, as estimated from electron paramagnetic resonance (EPR) and electron−nuclear double resonance (ENDOR) spectroscopy, has been debated over many years. While the EPR properties of the $P700^+$ signals initially were taken to indicate a dimeric state with approximately equal spin distribution within the radical (*13*, *14*), this interpretation was later questioned (*15*, *16*). More recently, ENDOR and electron spin echo envelope modulation (ESEEM) experiments have been interpreted to favor a decidedly asymmetrical spin distribution ranging from 3:1 to 10:1 (*17*−*21*), and even complete localization of the spin on a single Chl molecule (*22*). The latest ENDOR reports on this subject conclude that at least 85% of the spin in $P700^+$ is localized on a single Chl (*23*, *24*), and several recent reviews on the magnetic resonance properties of $P700^+$ concur with this view (*25*−*27*). With regard to the localization of the triplet state in ^{3}P700, magnetic resonance experiments with optical detection techniques have led to the conclusion that the triplet in ^{3}P700 is localized on the same molecule as the excess spin in $P700^+$ (*24*, *25*, *28*).

Fourier transform infrared (FTIR) difference spectroscopy is well suited to investigate the interaction of the Chl molecules with the surrounding protein as well as the electronic structure of P700, $P700^+$, and ^{3}P700. For example, the light-induced $P700^+$/P700 FTIR difference spectra of a series of PSI mutants of *Chlamydomonas* (*C.*) *reinhardtii* in which each of the conserved pairs of histidines located symmetrically on the PsaA and PsaB polypeptides that constitute the core of PSI is replaced by glutamines has led to the identification of the His axial ligand of each of the two Chl molecules of P700 (*29*). By combining the FTIR technique with global isotope labeling in the cyanobacterium *Synechocystis* sp. PCC 6803 (referred to in the following as *Synechocystis*), it was possible to discriminate the C═O vibrational modes of the Chl of P700 from those of the protein (*30*). A comparison of the $P700^+$/P700 and ^{3}P700/P700 FTIR difference spectra has led to the firm assignment of the C═O modes of the 9-keto and 10a-ester C═O groups from the two Chl molecules that constitute P700 (*30*). It was concluded that both carbonyl groups of one of the Chl's are free from interaction with the protein, while the two carbonyl groups of the other Chl engage in hydrogen-bonding interactions with the protein, leading, most notably, to an extreme frequency downshift ($\sim$60 cm^{-1}) of the 9-keto C═O group. It was also found that this asymmetry is maintained in the $P700^+$ state (*30*). Upon assuming comparable extinction coefficients for either the 9-keto or the 10a-ester C═O groups of the two Chl's, the relative amplitudes of their contribution in the $P700^+$/P700 spectra led to the conclusion that the positive charge in $P700^+$ is shared approximately equally between the two Chl molecules with a ratio between 1:1 and 2:1 (in favor of the Chl lacking the hydrogen bonds). Furthermore, the triplet state in ^{3}P700 was found to be fully localized on the Chl molecule that exhibits strong hydrogen-bonding interactions with the protein (*30*), a conclusion that is the opposite of that derived from magnetic resonance studies (*24*, *25*, *28*).

When the first X-ray structural model of PSI from the cyanobacterium *Synechococcus* (*S.*) *elongatus* at a resolution high enough to visualize the interactions between the Chl molecules and the surrounding amino acid residues appeared (*31*), it became clear that P700 is indeed a highly asymmetrical dimer made of one Chl *a* molecule with no hydrogen-bonding interactions with the PsaB polypeptide and one Chl *a*′ (the epimer of Chl *a* at the C_{10} position) with the 9-keto and the 10a- and 7c-ester C═O groups in hydrogen-bonding interactions with the PsaA polypeptide. Furthermore, the Mg atoms of both Chl molecules were found to interact with the Nτ nitrogen atom of the His residues previously proposed as axial ligands (*28*, *29*, *32*). The structural model of P700 (*31*) thus is in remarkably good agreement with the previous conclusions derived from the FTIR experiments (*30*, *33*). Additionally, it was excluded experimentally that the strong disagreement between the conclusions derived from FTIR and magnetic resonance studies could be due to the investigation of PSI preparations originating from different organisms or to differences in the temperature at which the experiments were performed in the various laboratories (*33*). However, these discrepancies were further highlighted by reports of ENDOR and absorption-detected magnetic resonance (ADMR) spectroscopy of mutants of the His axial ligands of P700 in *C. reinhardtii* which were taken to provide convincing evidence that the unpaired electron in $P700^+$ and the triplet state in ^{3}P700 are localized mainly on the Chl lying on the PsaB side (*25*, *28*). Moreover, the same description of the electronic structures of $P700^+$ and ^{3}P700 in wild-type *C. reinhardtii* PSI was maintained following optical and magnetic resonance spectroscopic studies of a mutant in which the Thr residue that forms a hydrogen bond with the 9-keto group of the PsaA Chl in the structural model of *S. elongatus* (*31*) was replaced by the non-hydrogen-bonding Val residue (*24*). Only in the mutant preparation was some evidence found that the distribution of the triplet state and of the spin over the two Chl's is affected.

The large discrepancy between the interpretation of the results of magnetic resonance and FTIR experiments led Hastings et al. (*34*) to analyze the $P700^+$/P700 FTIR difference spectra of *C. reinhardtii* and to propose an assignment of bands for the 9-keto C═O groups that differs considerably from the previous interpretation of the FTIR data (*30*) but that is more in line with the conclusions derived from magnetic resonance spectroscopy. However, the FTIR assignments in ref *34* are based on the perturbation of the 9-keto carbonyl frequency in a single mutant modified at the His axial ligand of the PsaA Chl, and they do not take into account the effect of global isotope labeling and the comparison of the $P700^+$/P700 and ^{3}P700/P700 FTIR difference spectra that were at the roots of the previous assignments (*30*). Furthermore, a comparable FTIR study of the effect of replacing one of the His axial ligands of the BChl's in the primary electron donor of the purple bacterium *Rhodobacter* (*Rb.*) *sphaeroides* by a variety of residues has

shown that the frequency of the BChl 9-keto and 10a-ester C═O groups of P could be significantly affected by such mutations owing probably to a repositioning of the primary donor within the cavity generated by the mutation (*35*). Therefore, the assignments proposed in ref *34* need to be reevaluated in light of these observations.

While seeking a way to investigate the distribution of the charge in the $P700^+$ oxidized dimer that would not involve the vibrations of the Chl's themselves, we considered the possibility of analyzing by FTIR difference spectroscopy the perturbation upon P700 photooxidation of the vibrational modes of the His residues that interact with the Mg atoms of the Chl dimer in P700. The C_5–Nτ stretching mode of the imidazole ring of histidine is a good candidate for such studies as it gives rise to a relatively strong band in an easily accessible region around 1100 cm^{-1} (*36*, *37*). Furthermore, ESEEM experiments using PSI complexes in which the His residues were isotopically labeled with ^{15}N have shown conclusively that a His residue interacts with the unpaired electron in $P700^+$ (*38*). In the present work, $P700^+$/P700 FTIR difference spectra of PSI core complexes from *Synechocystis* labeled either globally with ^{15}N or more selectively with [U-^{13}C]histidine have led to the identification of a differential signal corresponding to the downshift upon P700 photooxidation of the C_5−Nτ stretching mode of the imidazole ring. The amplitude of this signal is reduced by approximately half in PSI complexes from several mutants of *Synechocystis* in which the His PsaB 651 axial ligand of the Chl *a* molecule in P700 is replaced by other residues. This observation provides further evidence in favor of a symmetrical charge distribution within the two Chl molecules in $P700^+$.

MATERIALS AND METHODS

PSI core complexes from *Synechocystis* sp. PCC 6803 used for the ^{15}N labeling experiments were isolated according to ref *39*. Global isotope labeling with ^{15}N was obtained by replacing the sodium nitrate by its isotopomer. In the case of labeling of the His residues, a histidine-tolerant strain of *Synechocystis* was used and the culture medium was supplemented with histidine either unlabeled or uniformly labeled with ^{13}C (Isotope Cambridge Laboratories, Massachusetts). In this case the isolation of PSI core complexes was performed according to ref *40*. The extent of labeling was >95% for ^{15}N (P. Sétif, personal communication) and about 85% for [U-^{13}C]histidine.

To generate mutations in the PsaB gene, the plasmid pGEM-3C+, which contains the C-terminal region of the PsaB gene, a resistance gene for chloramphenicol and ampicillin, and the 760-bp region downstream of the PsaB gene, was used. A PCR-based method was used to create the mutant recombinant DNAs using pGEM-3C+ as a template. To clone the amplified DNA, a fragment, the third PCR product, was digested with *Eag*I and *Apa*I and ligated into pGEM-3C+ that had been digested with the same enzymes. The amplified regions from the ligated pGEM-3C+ were sequenced completely to confirm the presence of desired mutations and to ensure the fidelity of *Taq* polymerase. Plasmid DNAs with appropriate recombinant constructions were used to transform the recipient strain PCRTΔB (a gift from Dr. Lee MacIntosh). Transformation of the recipient strain, selection of transformants, and segregation of mutants were performed under low light intensity (2−3 μmol m^{-2} s^{-1}) at 30 °C according to ref *41*. After segregation, the genomic DNAs were isolated from the mutant strains. The fragments containing the mutated sites were amplified by PCR, and the fragments were sequenced to confirm the mutations. The PS I complexes were purified according to a previously published method (*42*).

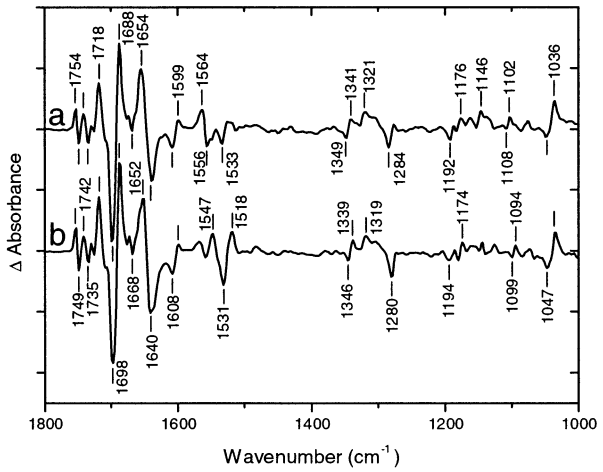

FIGURE 1: Light-induced $P700^+$/P700 FTIR difference spectrum of PSI core complexes from *Synechocystis* sp. PCC 6803 at 5 °C: (a) unlabeled PSI, (b) ^{15}N-labeled PSI. Each division on the vertical scale corresponds to 6×10^{-4} absorbance unit. About 100000 interferograms were added. The frequency of the bands is given ± 1 cm^{-1}. The spectral resolution is 4 cm^{-1}.

Samples for FTIR were prepared by centrifugation (300000*g* for 15 mn) of PSI complexes in Tris−HCl buffer (20 mM; pH 7.0) containing 20 mM sodium ascorbate and 50 μM methyl viologen. A small fraction of the resultant pellet was squeezed between two calcium fluoride windows, and the thickness of the sample was adjusted to give an absorption of about 0.8 OD unit at the maximum around 1650 cm^{-1}, with approximately half of this absorption being due to the amide I absorption and the other half to the scissoring mode of water. Light-induced difference spectra were recorded on Nicolet 60SX and 860 FTIR spectrometers at a temperature of 5 °C as previously reported (*30*).

RESULTS

Effect of Isotope Labeling on the $P700^+$/P700 FTIR Difference Spectra.

Figure 1 shows the $P700^+$/P700 FTIR difference spectra in the 1800−1000 cm^{-1} spectral range of PSI core complexes from *Synechocystis* that were either unlabeled (Figure 1a) or globally labeled with ^{15}N-labeled samples (Figure 1b). Similar spectra, measured at 90 K on the same PSI preparations, have been previously reported in the 1800−1200 cm^{-1} spectral range (*30*). Only limited effects are observed in the region above 1600 cm^{-1} where the C═O modes of Chl and of the amide I band absorb. This observation is consistent with (i) the absence of perturbation of the C═O modes of the isolated Chl upon labeling with ^{15}N (*30*) and (ii) the presence of a small coupling between the peptide C═O stretching and N−H bending modes, leading to a ^{15}N isotopic shift of about 3 cm^{-1} of the main amide I band in the absolute absorption spectrum (data not shown). The negative band at 1608 cm^{-1}, assigned to a C═

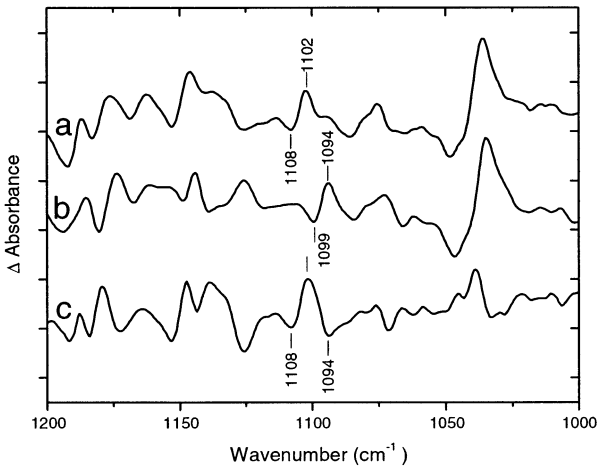

FIGURE 2: Light-induced $P700^+/P700$ FTIR difference spectrum of PSI complexes from *Synechocystis* at 5 °C: (a) unlabeled PSI, (b) ^{15}N-labeled PSI. (c) Double-difference spectrum, unlabeled minus ^{15}N-labeled. Each division on the vertical scale corresponds to 1.5×10^{-4} absorbance unit.

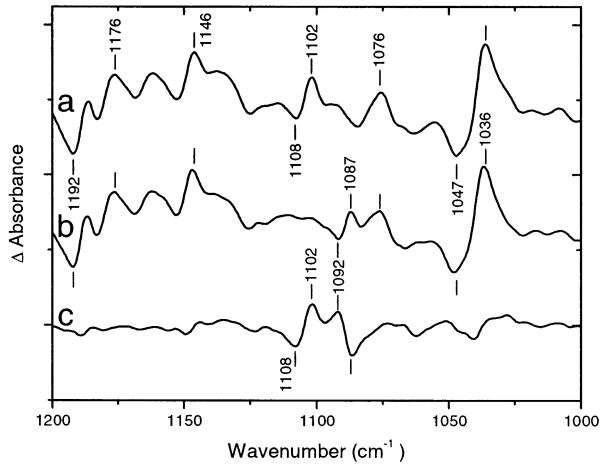

FIGURE 3: Light-induced $P700^+/P700$ FTIR difference spectrum at 5 °C of PSI complexes from a histidine-tolerant strain of *Synechocystis* containing (a) unlabeled histidine and (b) uniformly-^{13}C-labeled histidine. (c) Double-difference spectrum, unlabeled minus U-^{13}C-labeled. Each division on the vertical scale corresponds to 3×10^{-4} absorbance unit.

C marker mode for Chl with a pentacoordinated central Mg atom (*30*, *43*), is, as expected, unaffected by the labeling. Larger variations are observed in the region around 1550 cm^{-1} where the combined N−H and C−N amide II vibrational mode absorbs. In the 1200−1000 cm^{-1} spectral range, many positive and negative bands are affected by ^{15}N labeling (Figure 2). However, among those bands only one differential signal, negative at 1108 cm^{-1} and positive at 1102 cm^{-1}, appears in the ∼1090−1115 cm^{-1} frequency range that is characteristic of the "C_5−Nτ stretching" mode of histidine or 4-methylimidazole with a metal bound at the Nτ site and with the Nπ site either protonated or unprotonated (*37*). The ^{15}N isotopic downshift of the differential signal by 8−9 cm^{-1} is consistent with the calculated composition of this mode, which includes slightly more than 50% C_5−Nτ stretching vibration together with other ring deformation (mostly C−H) modes (*37*). The two latter observations indicate that the 1102/1108 cm^{-1} differential signal is likely to be contributed by the C_5−Nτ stretching mode of histidine. By combining attenuated total reflection and perfusion-induced FTIR difference spectroscopy (*44*, *45*), it has been verified that the 1102/1108 cm^{-1} differential signal observed in Figure 2a can be generated by changing the redox state of P700 chemically (data not shown) and therefore does not originate from photoreactions at the acceptor side.

A compelling confirmation that the ^{15}N-sensitive differential signal at 1102/1108 cm^{-1} in the $P700^+/P700$ FTIR spectrum (Figure 2a) originates from His residue(s) is obtained by comparing the $P700^+/P700$ FTIR difference spectra of PSI core complexes isolated from a culture of *Synechocystis* having incorporated histidine either unlabeled (Figure 3a) or uniformly labeled with ^{13}C (Figure 3b). In this case the 1102/1108 cm^{-1} differential signal is downshifted by 15−16 cm^{-1} for the [U-^{13}C]histidine, and the double-difference spectrum (Figure 3c) shows that this is the most affected mode in the 1200−1000 cm^{-1} spectral range. The downshift of the 1102/1108 cm^{-1} differential signal in the spectra of the unlabeled PSI (Figures 2a and 3a) leaves a frequency window with only smooth spectral features in the corresponding spectra of the isotopically labeled samples (Figures 2b and 3b), indicating the absence of overlapping modes of significant amplitude in the 1110−1095 cm^{-1} spectral region. This observation will prove useful in the analysis of the effects of mutating the His axial ligands of P700.

Effect of Mutations at His PsaB 651 on the $P700^+/P700$ FTIR Difference Spectra. The PsaB residue His 651 in *Synechocystis* (homologous to His 660 and His 656 in *S. elongatus* and *C. reinhardtii*, respectively), which acts as the axial ligand of the Chl *a* molecule of P700 with its carbonyl groups free from hydrogen bonds, has been replaced by the residue Cys, Gln, Leu, or Phe. Only the first three mutants have been investigated by FTIR difference spectroscopy, as the latter accumulates only very small amounts of PSI trimers. Their $P700^+/P700$ FTIR difference spectra in the 1800−1000 cm^{-1} spectral region are shown in Figure 4 together with the spectrum of the wild type (Figure 4a). The spectrum for each mutant has been normalized to that of the wild type by performing interactive subtraction (wild type minus mutant) and minimizing the residuals in the whole 1800−1000 cm^{-1} spectral range (data not shown). For the purpose of clarity, the expanded spectra are depicted in the spectral ranges 1800−1600 and 1200−1000 cm^{-1} in Figures 5 and 6, respectively. Before the specific perturbations of the spectrum elicited by each mutation are examined, it is worth recognizing that the main features as well as many smaller details of the $P700^+/P700$ FTIR difference spectra of wild-type PSI are maintained for all the mutants investigated. Notably, the 1608 and 1533 cm^{-1} marker modes for pentacoordinated Chl (*30*, *43*) in wild-type PSI (Figure 4a) are present in the spectra of all the mutants (Figure 4b−d). Similarly, the large spectral features assigned to the 9-keto and 10a-ester C═O groups of the two Chl's in P700 and $P700^+$ of wild-type PSI (Table 1) are present at almost the same frequency (within 1−2 cm^{-1}) in the mutant spectra (Figure 5).

When the spectrum in the 1800−1600 cm^{-1} range of the Cys mutant (Figure 5b) is compared to that of the wild type (Figure 5a), the large differential signals at 1718/1698 and 1654/1640 cm^{-1} that were previously assigned to the 9-keto

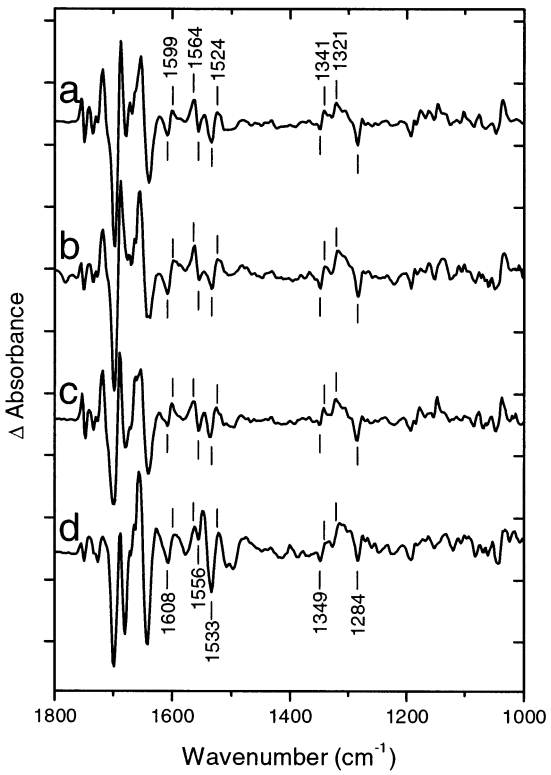

FIGURE 4: Light-induced $P700^+/P700$ FTIR difference spectrum of PSI complexes from *Synechocystis* at 5 °C: (a) wild type, (b) mutant HC(B651) in which His PsaB 651 is replaced by Cys, (c) mutant HQ(B651) in which His PsaB 651 is replaced by Gln, (d) mutant HL(B651) in which His PsaB 651 is replaced by Leu. Each division on the vertical scale corresponds to 6×10^{-4} absorbance unit.

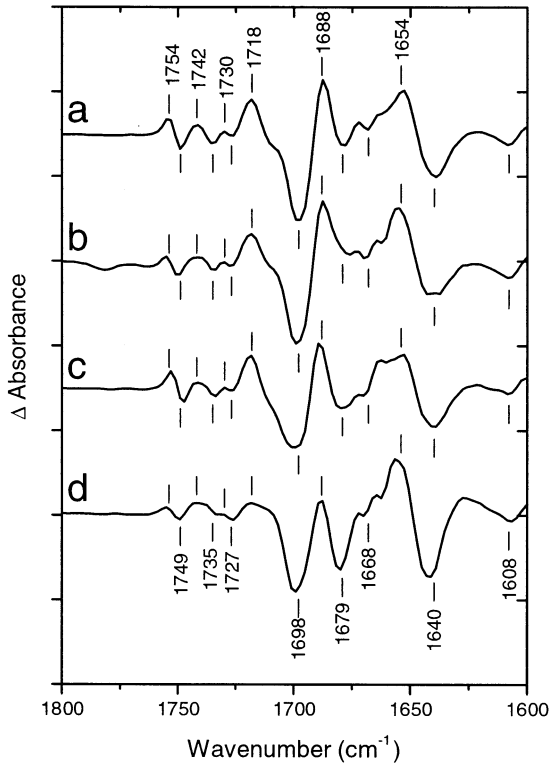

FIGURE 5: Light-induced $P700^+/P700$ FTIR difference spectrum of PSI complexes from *Synechocystis* at 5 °C: (a) wild type, (b) mutant HC(B651), (c) mutant HQ(B651), (d) mutant HL(B651). Each division on the vertical scale corresponds to 1.2×10^{-3} absorbance unit.

C═O group of the two Chl molecules in the $P700^+/P700$ FTIR difference spectrum of the wild type (*30*) are relatively little affected. The differential signals at 1754/1749 and 1742/1735 cm^{-1} assigned to the 10a-ester C═O in the spectrum of the wild type are somewhat reduced in amplitude in the mutant spectrum, but are not shifted significantly in frequency. In the case of the Gln mutant (Figure 5c), the amplitude and shape of the C═O ester absorption bands are essentially unperturbed compared to those of the wild type and only a small downshift ($1-2$ cm^{-1}) is observed. The 1718/1698 cm^{-1} differential signal becomes broader, while that at 1654/1640 cm^{-1} decreases slightly in amplitude. The spectrum of the Leu mutant (Figure 5d) is the most perturbed of the three mutant spectra with a small $1-2$ cm^{-1} upshift and an amplitude increase of the 1654/1640 cm^{-1} differential signal, while a larger decrease of the amplitude of the 1718/1698, 1742/1735, and 1754/1749 cm^{-1} differential signals is observed. The amplitude increase of the bands at 1679 and ~1550 cm^{-1} in the $P700^+/P700$ FTIR difference spectrum of the Leu mutant (Figure 4d) suggests a larger conformational change of the protein backbone upon P700 photooxidation in this mutant compared to both the wild type and the other mutants (Figure 4a−c).

In general, the main effect of the mutations is to alter the relative amplitude of the large differential signals at 1718/1698 and 1654/1640 cm^{-1} that were previously assigned to the upshift upon P700 photooxidation of the 9-keto C═O groups of the two Chl molecules in the $P700^+/P700$ FTIR difference spectrum of the wild type (*30*; Table 1). A similar effect is also observed in parallel on the relative amplitude of the differential bands attributed to the 10a-ester C═O groups (Figure 5). When the spectrum of the wild type is compared to those of the various mutants, these variations in the relative amplitudes of the differential signals can reach a factor of ~2. Besides changes of relative amplitudes, it can also be noticed that the perturbation of the shape of the differential signals appears to be slightly larger for the signal at 1718/1698 cm^{-1} than for that at 1654/1640 cm^{-1}. This suggests that mutating the His coordinated to the PsaB Chl affects the 9-keto C═O vibrational mode of this Chl slightly more than that of the PsaA Chl.

Table 1: Assignment of Carbonyl Stretching Frequencies (cm^{-1}) of the Two Chlorophylls of P700 in *Synechocystis* Sp. PCC 6803 at 5 °C

	carbonyl	P700	$P700^+$
Chl *a*′ (PsaA 676)	10a-ester	1735	1742
	9-keto	1640	1654
Chl *a* (PsaB 651)	10a-ester	1749	1754
	9-keto	1698	1718

In the spectral range $1200-1000$ cm^{-1} (Figure 6), the spectra of the mutants are significantly perturbed compared to that of the wild type, although many positive and negative bands still appear either at the same position or within close proximity. The largest spectral differences can be rationalized by considering that, compared to that of the wild type, each mutant spectrum contains modes from the new side chain that replaces His 651 and also from other residues whose local environments (and/or electrostatic interactions) are perturbed by the mutation. Nevertheless, the spectra in Figure 6 show that the 1102/1108 cm^{-1} differential signal previously assigned to the predominantly $C_5-N\tau$ stretching mode of

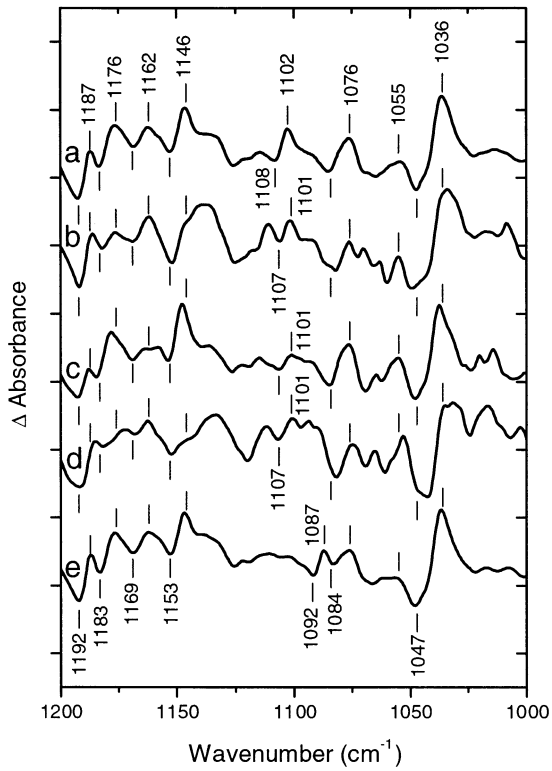

FIGURE 6: Light-induced P700$^+$/P700 FTIR difference spectrum of PSI complexes from *Synechocystis* at 5 °C: (a) wild type, (b) mutant HC(B651), (c) mutant HQ(B651), (d) mutant HL(B651), (e) wild-type PSI complexes containing uniformly-^{13}C-labeled histidine (same as Figure 3b). Each division on the vertical scale corresponds to 2.5×10^{-4} absorbance unit.

His residue(s) is still present in all of the mutants, albeit with a reduced amplitude and a small frequency downshift. This observation is strengthened when the differential features negative at 1107 cm^{-1} and positive at 1101 cm^{-1} of the PsaB mutant spectra (Figure 6b−d) are compared to the smooth traces in the 1110−1095 cm^{-1} regions of the isotopically labeled samples (Figures 2b and 6e). A closer analysis of the double-difference spectra, in which the spectrum of the U-^{13}C-labeled His sample (Figure 6e) is subtracted from each of the individual spectra in Figure 6a−d (data not shown but see the Supporting Information), indicates that the 1102/1108 cm^{-1} signal of the wild type (Figure 6a) is, in fact, the resultant of two differential signals of roughly equal amplitudes at ∼1101/1107 and approximately 1103/1109 cm^{-1}. We therefore assign these features to the C_5−Nτ mode of His PsaA 676 and PsaB 651, respectively. A more quantitative analysis of the frequency and amplitude of the differential signals of each of the two His residues will require the investigation by FTIR spectroscopy of mutants of the PsaA His axial ligand of P700 as well as of double mutants on both axial ligands.

DISCUSSION

PSI mutants on the His axial ligands of the P700 Chl molecules in *C. reinhardtii* have been investigated previously by FTIR difference spectroscopy. In the initial study aimed at the identification of the axial ligands of P700, each of the pairs of homologous His residues conserved in the PsaA and PsaB polypeptides was targeted and replaced by glutamines. Isolated PSI membranes were screened by FTIR difference spectroscopy, leading to the identification of PsaA 676 and PsaB 656 (analogous to PsaA 680 and PsaB 660, respectively in *S. elongatus*) as the axial ligands of P700 (*29*). An upshift and splitting of the 9-keto C═O band at 1700 cm^{-1} were observed in the HQ(A676)/HQ(B656) double mutant, and investigation of each of the corresponding single mutants showed that these new spectral features were primarily related to the HQ(A676) mutation. This work was further extended to a comparison of the P700$^+$/P700 FTIR difference spectra of PSI particles from *C. reinhardtii* bearing the mutation HL(B656) (*46*). Although most of the features of the P700$^+$/P700 FTIR difference spectra of wild-type PSI from *C. reinhardtii* are essentially the same for isolated particles and for membranes (*29*, *33*, *34*, *46*), the difference spectrum measured for particles of the HL(B656) mutant was appreciably more perturbed than the equivalent spectra obtained for *Synechocystis* (Figures 4a,d and 5a,d). It is not clear at present whether this difference is due to differences between the organisms or the respective protocols used for the isolation of the particles. More recently, the P700$^+$/P700 FTIR difference spectrum of PSI particles from the mutant HS(A676) in *C. reinhardtii* has shown an upshift and a splitting of the 9-keto C═O band at 1700 cm^{-1} (J. Breton and A. Weber, unpublished data; *34*) comparable to those reported for the HQ(A676) mutant (*29*).

Assignments of the Chl Carbonyl Vibrations in P700, P700$^+$, and ^{3}P700.

The perturbation of the 9-keto C═O band at 1700 cm^{-1} in the P700$^+$/P700 FTIR difference spectrum of PSI particles from the mutant HS(A676) in *C. reinhardtii* has recently been the basis of an assignment of the 9-keto C═O vibrations of the P700 Chl (*34*) that differs drastically from the previous assignment (*30*). Hastings et al. (*34*) propose that the 9-keto C═O groups of both Chl's in P700 contribute to the 1700 cm^{-1} band, with the PsaA and PsaB Chl of wild-type PSI absorbing at 1697 and 1702 cm^{-1}, respectively. They suggest that, upon P700$^+$ formation, the 1702 cm^{-1} band of P700 in the wild type upshifts by 14 cm^{-1} while the 1697 cm^{-1} band downshifts by 10 cm^{-1}. The HS(A676) mutation would only shift these frequencies by 1−3 cm^{-1} (*34*). To rationalize the different behavior of the 9-keto C═O groups of both Chl's upon P700 photooxidation, it was assumed that the charge is essentially localized on the PsaB Chl. While this would lead to a carbonyl frequency upshift of the PsaB Chl in P700$^+$, as observed for Chl cation formation in solution (*47*), the frequency downshift of the 9-keto C═O group of the PsaA Chl was proposed, admittedly, without experimental support (*34*). Such a downshift could possibly be attributed to an electrochromic effect on the PsaA Chl of the positive charge localized on the PsaB Chl, as has been proposed for the P$^+$/P FTIR spectra of hydrogen-bonded heterodimer mutants in *Rb. sphaeroides* (*48*). However, a downshift of the 9-keto C═O vibration of the PsaA Chl is difficult to reconcile with the fact that the 10a-ester C═O group, also localized on ring V of the same Chl, is proposed to upshift from 1735 to 1742 cm^{-1} upon P700$^+$ formation in all the previous and current FTIR studies of P700 (photo)oxidation (*30*, *34*, *45*, *47*, *49*−*51*). Furthermore, the frequency of the 9-keto C═O vibration of the PsaA Chl at 1697 cm^{-1} is already high for a free keto group and is not compatible with the hydrogen bond described in the structural model of *S. elongatus* (*31*). Finally, Hastings et al. (*34*) assign the large

differential signal at 1652/1636 cm^{-1} in the $P700^+$/P700 FTIR difference spectra of *C. reinhardtii*, which is equivalent to the 1654/1640 cm^{-1} signal of *Synechocystis* (*33*, *34*), to an imidazolium C_4═C_5 vibration of His PsaA 676 and His PsaB 656. As the 1654/1640 cm^{-1} signal of *Synechocystis* is left essentially unaffected upon U-^{13}C labeling of all the His residues (data not shown), the latter interpretation can be ruled out.

While the assignment scheme for the 9-keto C═O groups of the P700 Chl proposed by Hastings et al. (*34*) has been tailored to fit the view of the localization of the spin in $P700^+$ and of the triplet state in ^{3}P700 on the PsaB Chl currently derived from magnetic resonance experiments (*23*−*25*), it leaves aside the two essential sets of experiments that formed the basis of the previous assignments (*30*). First, global isotope labeling with either ^{2}H or ^{15}N in *Synechocystis* allowed the protein C═O vibrations to be distinguished from the 9-keto and 10a-ester C═O vibrations of the Chl in the $P700^+$/P700 FTIR difference spectrum of PSI particles. In addition, a comparison of the $P700^+$/P700 and ^{3}P700/P700 FTIR difference spectra allowed the vibrations of the 9-keto and 10a-ester C═O vibrations of the Chl in the P700 ground state to be unequivocally resolved for the first time. This in turn led to the firm assignment of the carbonyl vibrations in $P700^+$ and in ^{3}P700. It was further concluded that the ^{3}P700 triplet is fully localized on a Chl molecule that has the 9-keto and 10a-ester C═O groups both hydrogen-bonded to the protein, while the positive charge in $P700^+$ is shared between the latter Chl and another Chl with the 9-keto and 10a-ester C═O groups both free from interactions (*30*). These assignments, which are summarized in Table 1, were easily accommodated in the crystallographic model of P700 (*31*) by establishing the correspondence between the Chl molecule with the C═O groups with hydrogen bonds in the FTIR difference spectra and the PsaA Chl in the structural model (*33*).

Effect of the Mutations at the His Axial Mg Ligands on the Chl Vibrations in Synechocystis. Replacement of the PsaB His axial ligand of the Chl *a* molecule in P700 by Cys, Gln, or Leu induces only very small perturbations of the frequency of the Chl vibrations in the $P700^+$/P700 FTIR difference spectra (Figures 4 and 5). Each mutation generates some specific changes in the relative amplitudes of the bands assigned to the 10a-ester and 9-keto C═O stretching modes of the two Chl molecules of P700 (see Table 1), suggesting some changes in the distribution of the positive charge in $P700^+$ upon mutation. However, none of these changes provide evidence of large modifications of the structure or environment of P700 in either its neutral or its oxidized state. Much larger perturbations of the spectrum are seen in analogous Leu mutants in the RC of *Rb. capsulatus* and *Rb. sphaeroides* where the mutations result in formation of BChl−bacteriopheophytin heterodimers (*35*, *52*), and similarly large changes might be expected if the $P700^+$ charge is localized on a single Chl. The conclusion that the charge of $P700^+$ is delocalized is supported by the presence of a broad positive band around 3000 cm^{-1} in the $P700^+$/P700 FTIR difference spectra of the mutants (data not shown). As previously reported for wild-type *Synechocystis*, such an electronic transition would not be expected if $P700^+$ were monomeric (*30*, *33*). Finally, the Chl C═C modes at 1608 and 1533 cm^{-1}, which are characteristic of pentacoordination of the central Mg atom (*30*, *43*), are left unperturbed by the mutations, indicating that in each mutant a fifth axial ligand must replace the mutated His residue. At least for the Leu mutant, a water molecule probably takes the place of the His side chain, as originally proposed for *Rb. sphaeroides* RC mutants in which the His axial ligands of the BChl molecules of P were replaced by Gly (*53*).

Light-induced FTIR difference spectra of the photooxidation of P in *Rb. sphaeroides* have been investigated in a series of mutants of His M202, which is the axial ligand of the BChl interacting with the M-polypeptide (*35*). While Leu and Glu mutations led to heterodimeric primary donors, Gly, Ser, Cys, and Asn mutants showed FTIR spectra characteristic of homodimeric BChl−BChl primary donors. Compared to that of the wild type, however, these spectra exhibit small perturbations of the 10a-ester and 9-keto C═O vibrations for both P and P^+. Surprisingly, these perturbations of the frequency and the intensity of the bands do not affect specifically the BChl molecule on the M-side, but rather are observed on both BChl molecules of the primary donor. This effect has been related to the sensitivity of the BChl C═O groups on ring V to the local environment and the charge density on ring V, and is thought to reflect small molecular rearrangements of the BChl macrocycles and/or their substituents upon mutation (*35*). These variations probably are caused by slight displacements of the whole dimer that allow ligation of the Mg atom to the newly introduced side chain or, as previously proposed for the HG(M202) mutant (*53*), to a water molecule. It is therefore proposed that the variations in the frequency and intensity of the 9-keto and 10a-ester C═O bands of Chl observed in the $P700^+$/P700 FTIR difference spectra of all the His axial ligand mutants of *Synechocystis* (Figures 4 and 5) as well as of *C. reinhardtii* (*29*, *34*, *46*) are due primarily to repositioning of the P700 dimer in the protein cavity generated by the mutation. The same proposal also can explain how two equivalent mutations, such as HQ(B656) in *C. reinhardtii* and HQ(B651) in *Synechocystis*, have somewhat different effects on the $P700^+$/P700 FTIR difference spectra in different species (*29*; Figure 5c). Minute differences in the shape of the protein cavity for P700 in the two species can become important factors for the conformation and/or environment of the Chl carbonyl groups.

Effect of the Mutations at His PsaB 651 on the C_5–Nτ His Vibration. The first suggestions based on experimental results that a His residue acts as the axial ligand of Chl in P700 came from ENDOR and ESEEM spectroscopy on PSI of *Synechocystis* containing ^{15}N-labeled His (*38*) and from biophysical characterization of the mutant HQ(B656) in *C. reinhardtii* (*32*). It was later shown that the two homologous His residues PsaA 676 and PsaB 656 in *C. reinhardtii* were indeed the axial ligands of the two Chl molecules in P700 (*28*, *29*). In the X-ray structural model at 2.5 Å resolution of PSI of *S. elongatus*, the Mg atom of each Chl molecule of P700 is located 2.3 Å from the Nτ atom of the imidazole ring of the proximal His ligand, while the Mg···Mg distance in P700 is 6.3 Å (*31*). A positive charge on the macrocycle of a given Chl molecule in $P700^+$ therefore would be expected to affect the frequency of the C_5−Nτ imidazole stretching mode of the proximal His ligand much more than that of the His ligand of the second Chl molecule.

Histidine side chains are involved at the catalytic site in many biological reactions. The two nitrogen atoms of the imidazole group, which can achieve different protonation states at physiological pH, play a role as hydrogen bond donors or acceptors, in proton-transfer reactions, and in the binding of metals. FTIR spectroscopy is well suited to investigate the protonation and ligation states of His side chains in proteins, and the IR absorption properties of 4-methylimidazole as a model for the side chain of histidine have therefore been extensively investigated both experimentally and by quantum chemical calculations (*36*, *37*, *54*−*57*). The relatively intense $C_5-N\tau$ stretching band around 1100 cm^{-1} was found to be a good marker of the protonation and coordination state of the histidine side chain. In the absence of coordination to a metal, the IR frequency range observed for this mode is different for each protonation state of $N\tau$ and $N\pi$ and decreases in the order $N\tau$, $N\pi H > N\tau$, $N\pi \geq N\tau H$, $N\pi H \geq N\tau H$, $N\pi$ (*36*). When a metal is coordinated at $N\tau$, the $C_5-N\tau$ stretching mode also depends on whether the $N\pi$ site is protonated and occurs in the characteristic ranges of ∼1115−1100 and ∼1100−1090 cm^{-1}, respectively (*37*).

Bands corresponding to the $C_5-N\tau$ stretching mode of histidine side chains coordinated to a metal atom have been assigned by FTIR difference spectroscopy in several types of photosynthetic reactions involving the change of the redox state of either the metal itself or its immediate surroundings. In photosystem II reactions, a negative band occurs at 1104 cm^{-1} in spectra of the oxidation of cytochrome b_{559} (*54*), differential signals with bands negative at ∼1102 cm^{-1} and positive at 1111 cm^{-1} have been reported in the photoreduction of the oxidized non-heme iron atom (*58*−*60*), and a differential signal with bands negative at 1102 cm^{-1} and positive at 1109 cm^{-1} has been observed upon reduction of the primary quinone acceptor QA (*61*). A comparable signal with bands negative at 1101 cm^{-1} and positive at 1107 cm^{-1} occurs upon reduction of QA in *Rb. sphaeroides* RC's (*62*). For histidine residues that probably are coordinated to a Mn atom of the oxygen-evolving complex, the $C_5-N\tau$ stretching mode is found at 1113 cm^{-1} (*57*). The frequencies of ∼1107 and ∼1109 cm^{-1} found for the $C_5-N\tau$ stretching mode of the P700 histidines PsaA 676 and PsaB 651 thus fall in the middle of the range characteristic of histidine side chains protonated at the $N\pi$ site and coordinated to a metal atom (*37*).[2] The $C_5-N\tau$ modes of His PsaA 676 and PsaB 651 both exhibit an apparent downshift of 6 cm^{-1} upon photooxidation of P700. In contrast, the $C_5-N\tau$ mode of His M219 in *Rb. sphaeroides* and His D2−215 in PSII gives rise to apparent upshifts of 6−7 cm^{-1} upon QA reduction (*61*, *62*). Whether the change of the bond order of the $C_5-N\tau$ mode leading to these frequency shifts of opposite signs is due to a pure electrostatic effect of the nearby charge, to a change of electron density on the imidazole ring mediated through the coordinating metal, or to a combination of such effects remains to be clarified.

[2] The $C_4=C_5$ imidazole stretching mode is also a good marker for the state of protonation and coordination of His (*37*). In P700, this mode is observed at ∼1611 cm^{-1} with an amplitude about 1.5−2 times that of the 1108 cm^{-1} $C_5-N\tau$ mode (data not shown). This frequency is slightly above but close to the upper limit of the 1606−1593 cm^{-1} frequency range characteristic of His protonated at the $N\pi$ site and coordinated to a metal atom at $N\tau$ (*37*).

The interpretation of the FTIR data as showing a rather symmetrical distribution of the positive charge on the two Chl molecules in $P700^+$ (*30*, *33*) rests on the reasonable assumption that the extinction coefficients for the 9-keto and 10a-ester C=O groups of the two Chl molecules of P700 are not vastly different due to differences in their hydrogen-bonding state, environment, or chemical nature (*31*). The present results circumvent this concern by showing that the $C_5-N\tau$ modes of each of the His axial ligands of the two Chl molecules in P700 are also perturbed to a similar extent upon $P700^+$ formation, although the histidines are not conjugated to the Chl macrocycles. This observation provides independent and compelling evidence to reinforce our conclusion that the charge in $P700^+$ is distributed approximately equally over the two Chl molecules of the PSI primary electron donor (*30*, *33*).

The $P700^+$/P700 FTIR difference spectra of the three mutants in which His PsaB 651 is replaced by Cys, Gln, or Leu show only very small shifts (at most 2 cm^{-1}) of the frequency of Chl carbonyl vibrations compared to that of the wild type (Figure 5). Therefore, the hydrogen-bonding status of these C=O groups in both the neutral and oxidized states of P700 appears robust to changes of the axial ligand. However, the relative amplitude of the differential signals assigned to frequency upshifts of the 9-keto and 10a-ester C=O groups of the P700 Chl upon photooxidation (see Figure 5 and Table 1) varies within a factor of ∼2 as a function of the mutation, clearly suggesting that the charge distribution between the two halves of $P700^+$ is affected by the nature of the residue that replaces the His PsaB 651 axial ligand. To perform a more quantitative analysis of the charge distribution in $P700^+$, it will be necessary to compare the relative perturbations of the Chl carbonyl groups and the $C_5-N\tau$ mode of the remaining His axial ligand in the various mutants. Such a quantitative analysis by FTIR spectroscopy will require investigation of a series of His PsaA 676 mutants as well as of double mutants on both of the P700 axial ligands.

Comments on the Recent FTIR Study of the Thr (A739) Mutants of C. reinhardtii. After submission of the present work, a study by Witt et al. has appeared (*63*) that extends the initial characterization of the TV(A739) mutant of *C. reinhardtii* (*24*) to include a Tyr or a His mutation at the same Thr site. Besides studies by optical and magnetic resonance spectroscopy, the $P700^+$/P700 FTIR difference spectra are also reported. All three mutations induce large perturbations of the wild-type spectrum in the 1720−1600 cm^{-1} frequency range. Smaller effects are observed in the region 1730−1760 cm^{-1}, probably at least in part as a consequence of the normalization procedure that is constrained to this small frequency window. While the positive band at ∼1688 cm^{-1} in the spectrum of the wild type increases its amplitude by more than a factor of 2 in those of the three mutants, even larger perturbations are found between 1680 and 1620 cm^{-1}, with the spectrum of each mutant differing from that of the wild type (*63*). Notably, a positive band at 1656 cm^{-1} in the spectrum of the wild type is replaced by a negative band at 1657 cm^{-1} of comparable amplitude in that of TY(A739) and of much reduced amplitude in that of TH(A739). The negative band at 1634 cm^{-1} in the spectrum of the wild type appears to decrease slightly in amplitude and to downshift by ∼5 cm^{-1} in that

of TY(A739), is absent in that of TH(A739), and is reduced in amplitude in that of TV(A739). A very small negative band appears at 1669 cm^{-1} in the spectrum of TH(A739) and a larger one at 1672 cm^{-1} in that of TV(A739). It is essential to note that all these spectral alterations upon mutation occur within the main range of the amide I C═O vibrations and should be related, at least in part, to protein conformational changes. The mutated Thr is described in the structural model of P700 as interacting in a very specific way not only with the 9-keto carbonyl of the PsaA Chl but also with a water molecule that is hydrogen-bonded to the protein via a Tyr and a Ser (*31*). This arrangement makes it likely that the response of the protein in the vicinity of the Thr A739 side chain to the positive charge on $P700^+$ could be affected by the nature of the residue at the A739 site. In the case of wild-type and mutant RC's from purple bacteria the P^+/P FTIR spectra have been shown to contain protein contributions attributed to the electrostatic effect of the positive charge on the nearby residues (*64*). For $P700^+/P700$ FTIR difference spectra, contributions from amide I and II vibrations have been detected by global isotopic labeling experiments (*30*) and can be seen in the spectra shown in Figure 1, notably by the large ^{15}N isotope effects observed around 1550 cm^{-1} under the main amide II band. In the analysis of P700 axial ligand mutants of *C. reinhardtii*, the differential signal negative at ~1635 cm^{-1} and positive at 1652 cm^{-1} is perturbed to various extents depending on the mutation (*29*, *34*, *46*), although the hydrogen bond between Thr A739 and the PsaA Chl is not supposed to be affected in these mutants. While only small frequency shifts (<5 cm^{-1}) and small variations of amplitude were observed for the HQ(A676) and HQ(B656) mutants compared to the wild type (*29*), larger effects are apparent in the spectrum of the HL(B656) mutant (*46*).[3] More recently, Hastings et al. have attributed the whole 1652/1636 cm^{-1} differential signal in their $P700^+/P700$ spectrum of wild-type *C. reinhardtii* to protein contributions from the two His axial ligands (*34*). Surprisingly, the possibility that the protein contributes to the IR absorption changes observed by Witt et al. in the 1620−1680 cm^{-1} frequency range was readily ignored, and the authors state that their observations provide the first direct evidence that the 1634 cm^{-1} band can be ascribed to the 9-keto group of the PsaA Chl (*63*). It should be stressed that, in the absence of isotope labeling experiments or of an analysis of $^3P700/P700$ FTIR difference spectra, it is not possible to discriminate between Chl 9-keto C═O and protein C═O groups in the whole range of the amide I absorption. Therefore, the data presented in ref *63* provide no direct clues to support their assignment of the 1634 cm^{-1} band to a Chl 9-keto C═O vibration.[4]

Although the $P700^+/P700$ FTIR difference spectra of the Thr A739 mutants reported by Witt et al. (*63*) do not provide an unambiguous assignment of the 9-keto C═O vibration of the PsaA Chl of P700, they can bring some supporting evidence in favor of the existence of a hydrogen bond to the 9-keto C═O group of this Chl in *C. reinhardtii*. Taken together with the firm assignment previously made for the 1635 cm^{-1} band to the 9-keto C═O vibrational mode of the PsaA Chl of P700 (*30*, *33*), the observation that this band is perturbed, at least to some extent, in all the Thr A739 mutants arguably can be considered as evidence that the hydrogen bond to this residue has been affected by the mutations. The extent of perturbation of the hydrogen bond to the PsaA Chl upon the mutations could be studied by analyzing the $^3P700/P700$ FTIR difference spectra of the mutants to detect frequency upshifts of the 9-keto C═O group of this Chl. Such studies are of interest to investigate the influence of the strength of the hydrogen bond to the 9-keto C═O group of the PsaA Chl in P700, $P700^+$, and $^3P700$ on the charge/spin distribution in $P700^+$ and $^3P700$.

Issue of the Distribution of Charge/Spin in $P700^+$ and $^3P700$. The work by Witt et al. using various optical and magnetic resonance spectroscopic techniques on the Thr A739 mutants (*63*) brings new light for a discussion of the stringent discrepancy between the interpretation of the FTIR and magnetic resonance results concerning the distribution of charge/spin in $P700^+$ and $^3P700$ in wild-type PSI. In brief, it is reported that the features of the $P700^+/P700$ ΔA and ΔCD spectra cannot be described by a model which takes into account the excitonically coupled dimer with only minor perturbations from the surrounding Chl. This has consequences on the previous conclusion that the triplet state is localized on the PsaB Chl (*25*, *28*), which was based on the assumption that only mutations primarily affecting the Chl which carries the triplet state should become visible in the triplet-minus-singlet spectrum. It is recognized that, owing to the necessity to take into account all the RC Chl's in the analysis of the ΔA spectra, straightforward conclusions can no longer be drawn from ADMR spectroscopy concerning the localization of 3P700 (*63*). It is also suggested that the observation that the $P700^+/P700$ and the $^3P700/P700$ ΔA spectra are affected in a similar way by each of the various mutations (*28*, *63*) indicates that the triplet state and the positive charge are located on the same Chl. It therefore follows from the statements in ref *63* that the new results of ADMR and ΔA spectroscopy of P700 no longer contradict the finding from FTIR spectroscopy that $^3P700$ is fully localized on the PsaA Chl (*30*, *33*).

It has been argued that the discrepancy between the interpretation of the ENDOR and FTIR results concerning the distribution of the spin/charge density over the two Chl molecules of $P700^+$ could be related to some differences in the IR extinction coefficient for the C═O groups of the two Chl molecules of P700 in the neutral and/or cation state (*28*, *63*). As discussed above, the observation that the $C_5-N\tau$ IR mode of each of the His axial ligands of the two Chl molecules in P700 is also perturbed to a similar extent upon $P700^+$ formation provides independent evidence to reinforce our earlier conclusion that the charge in $P700^+$ is distributed approximately equally over the two Chl molecules of the PSI primary electron donor (*30*, *33*). Therefore, the reason for the discrepancy has to originate from other sources. In

[3] In refs *29* and *46*, the absorption changes below 1690 cm^{-1} were not discussed in terms of contributions of protein or Chl carbonyl groups as the proper assignment work (*30*) had not been achieved at that time. The 1652/1635 cm^{-1} differential signal in the $P700^+/P700$ spectrum of *C. reinhardtii* has been assigned since to the upshift upon $P700^+$ formation of the 9-keto C═O group of the PsaA Chl by comparison with that of *Synechocystis* (*33*).

[4] Note that a frequency of 1634 cm^{-1} is unprecedented for a 9-keto C═O vibration of Chl and falls outside the range reported for the common aggregation states of Chl. As discussed previously (*30*), the very specific Chl−water−Chl polymer of Ballschmiter and Katz, which absorbs at 1638 cm^{-1}, is not a likely model for Chl in P700.

this respect it should be stressed that the authors of the analysis of the relevant ENDOR data on $P700^+$ have clearly stated the existence of some inherent difficulties in the interpretation of their results (*23*, *25*, *28*, *63*). Notably, while the assignment of a dimeric $P700^+$ species requires the detection of hyperfine coupling constants (hfc's) from both dimer halves, it is recognized that an assignment of the hfc's from the PsaA Chl has not been achieved so far (*23*, *25*, *63*). Instead a different approach was used whereby the hfc's of $P700^+$ are compared to those of Chl a^+ in organic solvent, although, according to refs *23* and *25*, this estimate is not very reliable since the electronic structure of Chl a^+ is influenced by the solvent, counterion, and temperature. This makes it difficult to decide whether the differences observed between the in vivo and in vitro systems reflect a delocalization of spin density between the two halves of $P700^+$ or a redistribution of spin density on a single macrocycle (*23*, *25*, *63*).

One additional complexity noticed in the analysis of the ENDOR data on the P700 axial mutants in *C. reinhardtii* is the unexpected observation that only the hfc's assigned to the methyl group attached to ring III of the Chl are affected in the His PsaB axial ligand mutants while the hfc's assigned to the methyl groups on rings I and II are not affected (*28*). This was taken to indicate a modification in the local environment of the ring III methyl group caused by a movement of the PsaB Chl or a change in its conformation. While no changes of hfc's were observed for the His PsaA axial mutants (*28*), further complications were noticed with the Thr A739 mutants where significant changes of the hfc's of the ring III methyl group were observed (*63*). For the first time a mutation affecting the PsaA Chl led to changes of the hfc's of the other half of the dimer, which, according to ref *63*, may be interpreted as a spin density shift from the PsaB to the PsaA Chl of $P700^+$ and indicate an electronic coupling between the two halves of the dimer in $P700^+$ of the wild type.

Our initial estimate of the charge distribution in $P700^+$ from FTIR measurements (*30*) was based on the perturbation upon P700 photooxidation of the 10a-ester and 9-keto C═O groups, which are partially and fully conjugated to the P700 Chl macrocycles, respectively. In contrast, the methyl groups detected by ENDOR spectroscopy are not conjugated to the Chl macrocycle, and therefore, their hfc's may not directly correlate with the spin distribution over the whole macrocycle. The hfc's of the methyl group on ring III being very sensitive to modifications of the neighboring exocyclic ring V (*28*), it is therefore conceivable that a small change of the geometry or of the local electrostatic interactions in this region of $P700^+$ upon various mutations may affect the minute amount of spin localized on this specific methyl group. Notably, the unusually strong downshift of the frequency of the 9-keto C═O group of the PsaA Chl indicates a drastic perturbation of ring V of this Chl. Such perturbation may be responsible for the difficulties in assigning the methyl group on ring III of the PsaA Chl.

ACKNOWLEDGMENT

J.B. is grateful to Eliane Nabedryk, Mariangela di Donato, Winfried Leibl, and Bill Parson for stimulating discussions.

SUPPORTING INFORMATION AVAILABLE

Calculation of the frequency and the relative amplitude of the differential signals assigned to the PsaA 676 and PsaB 651 His axial ligands of the P700 Chl. This material is available free of charge via the Internet at http://pubs.acs.org.

REFERENCES

1. Hoff, A. J., and Deisenhofer, J. (1997) *Phys. Rep. 287*, 1−248.
2. Deisenhofer, J., Epp, O., Sinning, I., and Michel, H. (1995) *J. Mol. Biol. 246*, 429−457.
3. Allen, J. P., Feher, G., Yeates, T. O., Komiya, H., and Rees, D. C. (1987) *Proc. Natl. Acad. Sci. U.S.A. 84*, 5730−5734.
4. Ermler, U., Fritzsch, G., Buchanan, S. K., and Michel, H. (1994) *Structure (London) 2*, 925−936.
5. Stowell, M. H. B., McPhillips, T. M., Rees, D. C., Soltis, S. M., Abresch, E., and Feher, G. (1997) *Science 276*, 812−816.
6. McAuley, K., Fyfe, P. K., Ridge, J. P., Cogdell, R. J., Isaacs, N. W., and Jones, M. R. (2001) *Biochemistry 39*, 15032−15043.
7. Allen, J. P., and Williams, J. C. (1995) *J. Bioenerg. Biomembr. 27*, 275−283.
8. Philipson, K. D., Sato, V. L., and Sauer, K. (1972) *Biochemistry 11*, 4591−4595.
9. Breton, J. (1977) *Biochim. Biophys. Acta 459*, 66−75.
10. den Blanken, H. J., and Hoff, A. J. (1983) *Biochim. Biophys. Acta 724*, 52−61.
11. Ikegami, I., and Itoh, S. (1988) *Biochim. Biophys. Acta 934*, 39−46.
12. Krawczyk, S., and Macsymiec, W. (1991) *FEBS Lett. 286*, 110−112.
13. Norris, J. R., Uphaus, R. A., Crespi, H. L., and Katz, J. J. (1971) *Proc. Natl. Acad. Sci. U.S.A. 68*, 625−628.
14. Norris, J. R., Scheer, H., Druyan, M. E., and Katz, J. J. (1974) *Proc. Natl. Acad. Sci. U.S.A. 71*, 4897−4900.
15. Wasielewski, M. R., Norris, J. R., Crespi, H. L., and Harper, J. (1981) *J. Am. Chem. Soc. 103*, 7664−7665.
16. O'Malley, P. J., and Babcock, G. T. (1984) *Proc. Natl. Acad. Sci. U.S.A. 81*, 1098−1101.
17. Davis, I. H., Heathcote, P., MacLachlan, D. J., and Evans, M. C. W. (1993) *Biochim. Biophys. Acta 1143*, 183−189.
18. Rigby, S. E. J., Nugent, J. H. A., and O'Malley, P. J. (1994) *Biochemistry 33*, 10043−10050.
19. Evans, M. C. W., Bratt, P. J., Heathcote, P., and Moënne-Loccoz, P. (1995) in *Photosynthesis: from Light to Biosphere* (Mathis, P., Ed.) Vol. II, pp 183−186, Kluwer, Dordrecht, The Netherlands.
20. Käss, H., and Lubitz, W. (1996) *Chem. Phys. Lett. 251*, 193−203.
21. Käss, H., Fromme, P., and Lubitz, W. (1996) *Chem. Phys. Lett. 257*, 197−206.
22. Mac, M., Bowlby, N. R., Babcock, G. T., and McCracken, J. (1998) *J. Am. Chem. Soc. 120*, 13215−13223.
23. Käss, H., Fromme, P., Witt, H. T., and Lubitz, W. (2001) *J. Phys. Chem. B 105*, 1225−1239.
24. Witt, H., Schlodder, E., Bordignon, E., Carbonera, D., Niklas, J., and Lubitz, W. (2001) *PS2001 Proceedings of the 12th International Congress on Photosynthesis*, S6-011, CSIRO Publishing, Collingwood, Victoria, Australia.
25. Weber, A., and Lubitz, W. (2001) *Biochim. Biophys. Acta 1507*, 61−79.
26. Deligiannakis, Y., and Rutherford, A. W. (2001) *Biochim. Biophys. Acta 1507*, 226−246.
27. Rigby, S. E. J., Evans, M. C. W., and Heathcote, P. (2001) *Biochim. Biophys. Acta 1507*, 247−259.
28. Krabben, L., Schlodder, E., Jordan, R., Carbonera, D., Giacometti, G., Lee, A. N., Weber, A. N., and Lubitz, W. (2000) *Biochemistry 39*, 13012−13025.
29. Redding, K., McMillan, F., Leibl, W., Brettel, K., Hanley, J., Rutherford, A. W., Breton, J., and Rochaix, J.-D. (1998) *EMBO J. 17*, 50−60.
30. Breton, J., Nabedryk, E., and Leibl, W. (1999) *Biochemistry 38*, 11585−11592.
31. Jordan, P., Fromme, P., Witt, H. T., Klukas, O., Saenger, W., and Krauss, N. (2001) *Nature 411*, 909−917.
32. Weber, A. N., Su, H., Bingham, S. E., Käss, H., Krabben, L., Khun, M., Jordan, R., Schlodder, E., and Lubitz, W. (1996) *Biochemistry 35*, 12857−12863.
33. Breton, J. (2001) *Biochim. Biophys. Acta 1507*, 180−193.

34. Hastings, G., Ramesh, V. M., Wang, R., Sivakumar, V., and Weber, A. (2001) *Biochemistry 40*, 12943−12949.
35. Nabedryk, E., Schulz, C., Müh, F., Lubitz, W., and Breton, J. (2000) *Photochem. Photobiol. 71*, 582−588.
36. Hasegawa, K., Ono T.-A., and Noguchi, T. (2000) *J. Phys. Chem. B 104*, 4253−4265.
37. Hasegawa, K., Ono T.-A., and Noguchi, T. (2002) *J. Phys. Chem. A 106*, 3377−3390.
38. Mac, M., Tang, X.-S., Diner, B. A., McCracken, J., and Babcock, G. T. (1996) *Biochemistry 35*, 13288−13293.
39. Bottin, H., and Sétif, P. (1991) *Biochim. Biophys. Acta 1057*, 331−336.
40. Tang, X.-S., and Diner, B. A. (1994) *Biochemistry* (1996) *33*, 4595−4603.
41. Sun, J., Xu, W., Hervás, M., Navarro, J. A., De La Rosa, M. A., and Chitnis, P. R. (1999) *J. Biol. Chem. 274*, 19048−19054.
42. Sun, J., Ke, A., Jin, P., Chitnis, V. P., and Chitnis, P. R. (1998) *Methods Enzymol. 297*, 124−139.
43. Fujiwara, M., and Tasumi, M. (1986) *J. Phys. Chem. 90*, 5646−5650.
44. Iwaki, M. Andrianambinintsoa, S., Rich, P. R., and Breton, J. (2001) *PS2001 Proceedings of the 12th International Congress on Photosynthesis*, S7-009, CSIRO Publishing, Collingwood, Victoria, Australia.
45. Iwaki, M. Andrianambinintsoa, S., Rich, P. R., and Breton, J. (2002) *Spectrochim. Acta A 58*, 1523−1533.
46. Leibl, W., Brettel, K., Nabedryk, E., Breton, J., Rochaix, J.-D., and Redding, K. (1998) in *Photosynthesis:Mechanisms and Effects* (Garab, G., Ed.) Vol. I, pp 595−598, Kluwer, Dordrecht, The Netherlands.
47. Nabedryk, E., Leonhard, M., Mäntele, W., and Breton, J. (1990) *Biochemistry 29*, 3242−3247.
48. Nabedryk, E., Breton, J., Williams, J. C., Allen, J. P., Kuhn, M., and Lubitz, W. (1998) *Spectrochim. Acta, A 54*, 1219−1230.
49. Tavitian, B., Nabedryk, E., M., Mäntele, W., and Breton, J. (1986) *FEBS Lett. 201*, 151−157.
50. Hamacher, E., Kruip, J., Rögner, M., and Mäntele, W. (1996) *Spectrochim. Acta, A 52*, 107−121.
51. Kim, S., and Barry, B. A. (2000) *J. Am. Chem. Soc. 122*, 4980−4981.
52. Nabedryk, E., Robles, S. T., Goldman, E., Youvan, D. C., and Breton, J. (1992) *Biochemistry 31*, 10852−10858.
53. Goldsmith, J. O., King, B., and Boxer, S. G. (1996) *Biochemistry 35*, 2421−2428.
54. Berthomieu, C., Boussac, A., Mäntele, W., Breton, J., and Nabedryk, E. (1992) *Biochemistry 31*, 11460−11471.
55. Berthomieu, C., and Boussac, A. (1995) *Biospectroscopy 1*, 187−206.
56. Majoube, M., Millié, P., and Vergoten, G. (1995) *J. Mol. Struct. 344*, 21−36.
57. Noguchi, T., Inoue, Y., and Tang, X.-S. (1999) *Biochemistry 38*, 10187−10195.
58. Hienerwadel, R., and Berthomieu, C. (1995) *Biochemistry 34*, 16288−16297.
59. Noguchi, T., and Inoue, Y. (1995) *J. Biochem. 118*, 9−12.
60. Berthomieu, C., and Hienerwadel, R. (2001) *Biochemistry 34*, 4044−4052.
61. Noguchi, T., Inoue, Y., and Tang, X.-S. (1999) *Biochemistry 38*, 399−403.
62. Breton, J., Richaud, P., Verméglio, A., and Nabedryk, E. (2001) *PS2001 Proceedings of the 12th International Congress on Photosynthesis*, S7-002, CSIRO Publishing, Collingwood, Victoria, Australia.
63. Witt, H., Shlodder, E., Teutloff, C., Niklas, J., Bordignon, E., Carbonera, D., Kohler, S., Labahn, A., and Lubitz, W. (2002) *Biochemistry 41*, 8557−8569.
64. Nabedryk, E. (1996) in *Infrared Spectroscopy of Biomolecules* (Mantsch, H. H., and Chapman, D., Eds.) pp 39−81, Wiley-Liss, New York.

BI0262404